

Crystallization and Melting Behavior of Nano-CaCO₃/Polypropylene Composites Modified by Acrylic Acid

Zhidan Lin, Zhenzhen Huang, Yu Zhang, Kancheng Mai, Hanmin Zeng

Materials Science Institute, College of Chemistry and Chemical Engineering, Key Laboratory for Polymeric Composites and Functional Materials of the Ministry of Education, Zhongshan University, Guangzhou 510275, China

Received 30 December 2002; accepted 23 June 2003

ABSTRACT: Nano-CaCO₃/polypropylene (PP) composites modified with polypropylene grafted with acrylic acid (PP-g-AA) or acrylic acid with and without dicumyl peroxide (DCP) were prepared by a twin-screw extruder. The crystallization and melting behavior of PP in the composites were investigated by DSC. The experimental results showed that the crystallization temperature of PP in the composites increased with increasing nano-CaCO₃ content. Addition of PP-g-AA further increased the crystallization temperatures of PP in the composites. It is suggested that PP-g-AA could improve the nucleation effect of nano-CaCO₃. However, the improvement in the nucleation effect of nano-CaCO₃ would be saturated when the PP-g-AA content of 5 phf (parts per

hundred based on weight of filler) was used. The increase in the crystallization temperature of PP was observed by adding AA into the composites and the crystallization temperature of the composites increased with increasing AA content. It is suggested that the AA reacted with nano-CaCO₃ and the formation of Ca(AA)₂ promoted the nucleation of PP. In the presence of DCP, the increment of the AA content had no significant influence on the crystallization temperature of PP in the composites. © 2003 Wiley Periodicals, Inc. *J Appl Polym Sci* 91: 2443–2453, 2004

Key words: poly(propylene) (PP); nanocomposites; crystallization; DSC; graft copolymers

INTRODUCTION

Polypropylene (PP) has been widely used for its good processing properties, high rigidity, and excellent mechanical properties. However, to meet various applications, further increased-use temperature and improved mechanical properties still constitute the main focus of PP modification. The incorporation of fillers into PP can lead to changes in crystallization and melting behavior of PP. According to the nucleation ability of the filler for the crystallization of PP, the fillers can be classified into two kinds, active and inactive. The nucleating effect of CaCO₃ on PP is drastically disputed, which relates to the crystal form, surface topography, and dispersion of CaCO₃. The addition of CaCO₃ with different crystal form and surface topography into PP results in various changes in the crystallization morphology, the proportion of crystallization phase to amorphous phase, and the distribution of these two phases, which accordingly affects the mechanical properties of CaCO₃/PP composites. Therefore, many studies on the crystallization and melting behavior of CaCO₃/PP composites have been reported.

There were reports that the addition of CaCO₃ markedly improved the nucleation effect and the crystallization temperature of PP attributed to the heterogeneous nucleation effect of CaCO₃.^{1,2} The increase in crystallization temperature was related to the particle size and content of CaCO₃; the smaller the size,³ the larger the amount of CaCO₃,⁴ and the more significant the improvement in crystallization behavior. Khare et al.⁵ found that the incorporation of CaCO₃ increased the crystallization rate of PP and decreased the spherulite size with the increase of the CaCO₃ content. The decreased crystallization half-time was observed with the increase of the CaCO₃ content, and was related to crystallization temperature. At high crystallization temperature, a greater decreased crystallization half-time was observed. Although the incorporation of CaCO₃ had no influence on the mechanism of crystallization nucleation, the crystallization temperature, crystallization rate, and Ozawa exponent of PP depended on the CaCO₃ content.⁶

The surface treatment of CaCO₃ with coupling agents, such as silane and titanate, could change the heterogeneous nucleation effect of CaCO₃ on PP. Albano et al.⁷ found that addition of CaCO₃ treated with and without titanate coupling agents increased the crystallization temperature of PP by about 7°C. CaCO₃ treated with silicone was more effective in increasing the crystallization degree of PP than that treated with titanate.⁸ The nucleation ability and the crystallization

Correspondence to: K. Mai.

TABLE I
Composition of Nano-CaCO₃/PP Composites

Sample	PP (wt %)	CC (wt %)	AA (phf) ^a	DCP (phf)	FPP (phf)
PP	100	—	—	—	—
CC2	98	2	—	—	—
CC5	95	5	—	—	—
CC10	90	10	—	—	—
CC40	60	40	—	—	—
CC40F5	60	40	—	—	5
CC40F10	60	40	—	—	10
CC40AA2	60	40	2	—	—
CC40AA4	60	40	4	—	—
CC40AA6	60	40	6	—	—
CC40AA2D	60	40	2	0.1	—
CC40AA4D	60	40	4	0.1	—
CC40AA6D	60	40	6	0.1	—

^a phf denotes parts per hundred based on weight of filler.

temperature decreased as PP was filled with CaCO₃ treated with oligomer of ethylene oxide.¹ Mitsubishi et al.⁴ studied the crystallization behavior of PP filled with CaCO₃ modified with alkyl dihydrogen phosphate and found that the shape and temperature of the crystallization peak of PP depended on the particle size of CaCO₃. For the CaCO₃ with particle sizes of 1 and 4.5 μm, double crystallization peaks of PP were observed. However, only a single peak was observed when the particle size was 30 μm. For the untreated CaCO₃, the crystallization temperature of PP increased with the increase of volume fraction of CaCO₃. CaCO₃ modified with plasma-polymerized acetylene

did not obviously change the crystallization and melting behavior of PP. However, the heat of fusion of PP filled with untreated CaCO₃ decreased with increase of the filler content and depended on the surface modification methods of CaCO₃. It was believed that the increase of the filler content distorted the crystalline structure and led to the change of microcrystalline orientation.⁹

In recent years, functionalized macromolecular coupling agents have been used to improve the interface interaction between CaCO₃ and PP. Rahma and Fella¹⁰ investigated the effect of the concentration of peroxide on the crystallization behavior of CaCO₃/PP

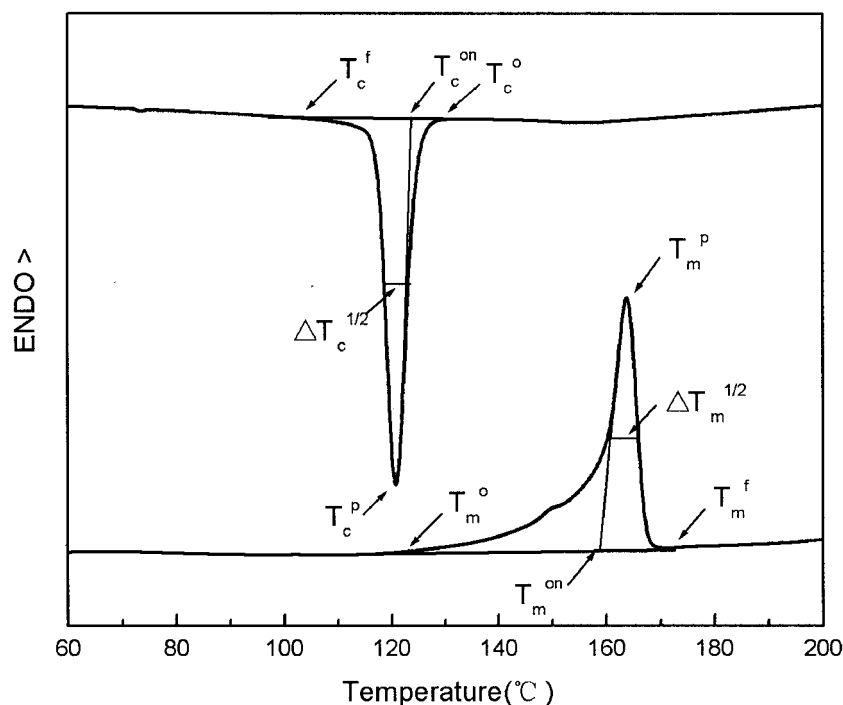


Figure 1 Determination of the crystallization and melting parameters.

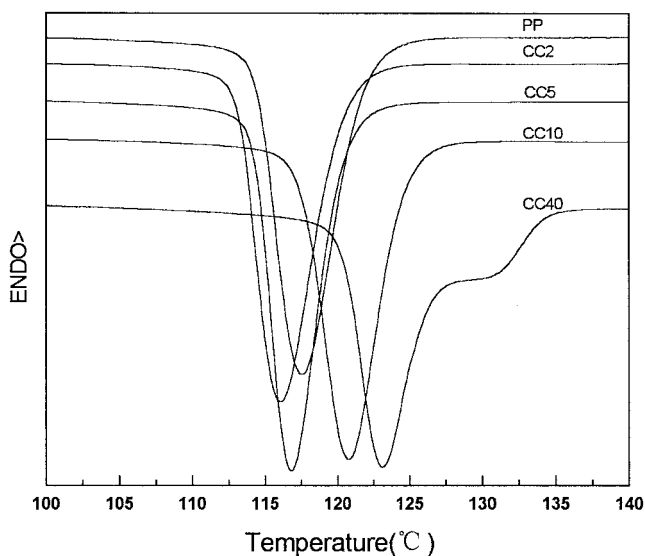


Figure 2 DSC crystallization curves of PP and nano-CaCO₃/PP.

composites modified by polypropylene grafted with acrylic acid (PP-*g*-AA). The result showed that the melting point of PP decreased rapidly with peroxide content initially, but then leveled off at peroxide content of 0.6 phr (parts per hundred based on weight of resin) because of the degradation of PP. This phenomenon was attributed to two competitive effects: (1) β -chain scission produced short chains and increased the crystallization rate; (2) the increase in the free radicals produced by high content of peroxide increased the chance of chain termination and the molecular weight and thus decreased the crystallization rate. Tabtiang and Venables² also investigated the effect of the content of AA, dicumyl peroxide (DCP), and the stabilizer TMP on the crystallization behavior of CaCO₃/PP. The result suggested that the increase of the content of DCP and TMP decreased the crystallization temperature of PP, but the crystallization temperature increased with increasing AA content. It was suggested that the TMP with a weak nucleation ability covered the fringe nucleation sites of CaCO₃ crystal

and decreased the heterogeneous nucleation effects of CaCO₃. On the contrary, an increased crystallization temperature of PP was observed as the AA and DCP were added together, which was attributed to the nucleation of Ca(AA)₂ formed in the process of material preparation. Both AA and TMP reacted competitively with polymeric PP free radicals initiated by DCP as the AA, TMP, and DCP were all added to PP. The increase in the concentrations of TMP and DCP decreased the crystallization temperature of PP. Moreover, the increase in the AA content increased the crystallization temperature of PP because of the formation of the higher nucleation ability of Ca(AA)₂.

Tabtiang and Venables¹¹ further investigated the performance of several unsaturated acids and acid anhydrides of varying molecular weight for CaCO₃ filler in PP. The modified CaCO₃ were then compounded with polypropylene, both in the presence and absence of an initiator, through twin-screw extrusion to give compounds containing 75 phr of CaCO₃. Infrared analyses showed that reaction between each coating and the CaCO₃ surface led to the formation of carboxylate salts. The occurrence of peroxide initiated transfer grafting between the alkenyl chains of the coatings and the PP matrix during compounding was inferred from extraction studies and from physical test data. Extensive grafting was evident for the AA-coated filler, but much less so for coatings with longer alkenyl chains. In the presence of peroxide the melt flow rates of each compound increased because of the reduction of molecular weight of the matrix polymer as a consequence of free radical-induced grafting and degradation reactions. This led to the reduction in toughness and ductility of compounds with surface coatings that possessed alkenyl chains with fewer than 17 carbon atoms. For those with chains lengths of 17 or greater, toughness was substantially improved as a result of the release of matrix constraint around the filler particles that counteracted the effects of degradation.

With the development of nanotechnology, new polymeric composites filled with nanofillers have been rapidly developed.¹²⁻²⁶ The mechanical properties of

TABLE II
DSC Crystallization Results of PP and Nano-CaCO₃/PP^a

Sample	T_c^0 (°C)	T_c^p (°C)	T_c^f (°C)	T_c^{on} (°C)	ΔH_c (J/g)	ΔT_c^1 (°C)	ΔT_c^2 (°C)	$\Delta T_c^{1/2}$ (°C)
PP	128.2	117.5	99.3	121.9	101.1	28.9	4.3	4.5
CC2	127.9	116.1	97.3	120.4	99.5	30.5	4.4	4.3
CC5	126.8	116.8	95.7	120.4	103.2	31.1	3.6	3.5
CC10	129.6	120.8	103.2	124.6	97.7	26.4	3.8	4.3
CC40	137.5	123.1	98.2	127.1	111.5	39.3	4.0	4.3

^a T_c^0 , the temperature at which crystallization curve deviates from the baseline; T_c^p , the peak temperature of crystallization; T_c^f , the temperature at the completion of crystallization; T_c^{on} , the temperature at the onset of crystallization; $\Delta T_c^1 = T_c^0 - T_c^f$, the width of the crystallization peak; $\Delta T_c^2 = T_c^{on} - T_c^p$, the width of the crystallization peak in the high temperature region; $\Delta T_c^{1/2}$, the half-height width of crystallization peak; ΔH_c , the heat of crystallization.

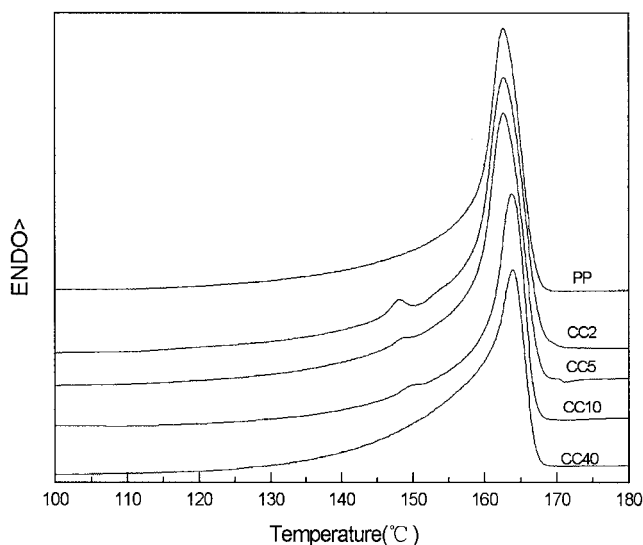


Figure 3 DSC melting curves of PP and nano-CaCO₃/PP.

polymeric materials depend on the crystallization behavior of the polymeric matrix, so there were some reports on the crystallization behavior of PP filled with nanomaterials. Xu et al.²⁷ studied the nonisothermal crystallization kinetics of polypropylene/montmorillonite (MMT) nanocomposites. The result showed that the crystallization temperature shifted to a higher temperature. At the same cooling rate, the crystallization temperature of the PP nanocomposite was higher than that of pure PP, and the Avrami exponent of the nanocomposite was less than that of pure PP. The incorporation of the organic MMT decreased the crystallization activation energy of PP. It was believed that nano-MMT had a heterogeneous nucleation effect during the crystallization process of PP. Studies^{28,29} on the isothermal crystallization kinetics of the PP/MMT nanocomposite also indicated that MMT had an obvious heterogeneous nucleation effect on PP and markedly increased the crystallization rate of PP. The Avrami exponent was $\cong 3.0$. It was suggested that the crystallization of PP nanocomposites occurred on the typical mechanism of heterogeneous nucleation.

The effect of nanoparticles on the crystallization behavior of PP was also investigated. Addition of nano-SiO₂ significantly increased the crystallization temperature of PP in PP/EPDM composites because of the heterogeneous nucleation effect of nano-SiO₂.³⁰ The nucleation effect of nanoparticles was related to the particle size.³¹ In the system of PP/nano-Ca₃(PO₄)₂, the decrease in particle size and the increase in the active surface area increased the heterogeneous nucleation effect and the crystallization rate of PP.

Nano-CaCO₃ significantly improved the nucleation of PP, which is different with micro-CaCO₃. Wang and Huang³² studied the effect of nano-CaCO₃ on the crystallization property of PP. The onset crystallization temperature of PP was increased slightly with increasing nano-CaCO₃ content and the heat of fusion initially increased and then fell. For the nano-CaCO₃ content below 3.5 wt %, nano-CaCO₃ dispersed well in the PP matrix and reinforced the interface interaction between matrix and nano-CaCO₃, which significantly induced the heterogeneous nucleation of PP and increased the degree of crystallization. For the nano-CaCO₃ content above 3.5 wt %, the heterogeneous nucleation effect and the degree of crystallization of PP decreased because of the severe aggregation of nano-CaCO₃. The heat of fusion of PP in its composites filled with nano-CaCO₃ was higher than that of the composites filled with micro-CaCO₃ as a result of the high heterogeneous nucleation effect of nano-CaCO₃. The melting behavior of nano-CaCO₃/PP composite was also investigated by Ren.³³ For the pure PP, a melting peak of the α -crystal was observed. For nano-CaCO₃/PP, there was not only a melting peak of the α -crystal at 165°C, but also a small peak at 150.6°C, which corresponded to the β -crystal. It was suggested that the nano-CaCO₃ induced the formation of a few β -crystals of PP. The smaller the nanoparticles, the greater the heterogeneous nucleation effect of β -crystallization.

To develop polymeric composites modified with nanomaterials, it is most important to resolve some problems, such as dispersion of nanomaterials in the

TABLE III
DSC Melting Results of PP and Nano-CaCO₃/PP^a

Sample	T_m^0 (°C)	T_m^p (°C)	T_m^f (°C)	T_{on}^n (°C)	ΔH_m (J/g)	ΔT_m (°C)	$\Delta T_m^{1/2}$ (°C)
PP	110.0	162.7	170.9	158.9	101.0	60.9	5.1
CC2	112.7	162.7	171.8	158.1	98.7	59.1	5.9
CC5	112.1	162.7	171.4	158.3	104.1	59.1	5.9
CC10	116.1	163.9	172.1	159.6	90.8	56.0	4.5
CC40	113.2	164.0	169.8	158.6	106.8	56.6	6.7

^a T_m^0 , the temperature at which melting curve deviates from the baseline; T_m^p , the peak temperature of melting curve; T_m^f , the temperature at the completion of melting; T_{on}^n , the temperature at the onset of melting curve; $\Delta T_m = T_m^f - T_m^0$, the width of the melting peak; $\Delta T_m^{1/2}$, the half-height width of melting peak; ΔH_m , the heat of fusion.

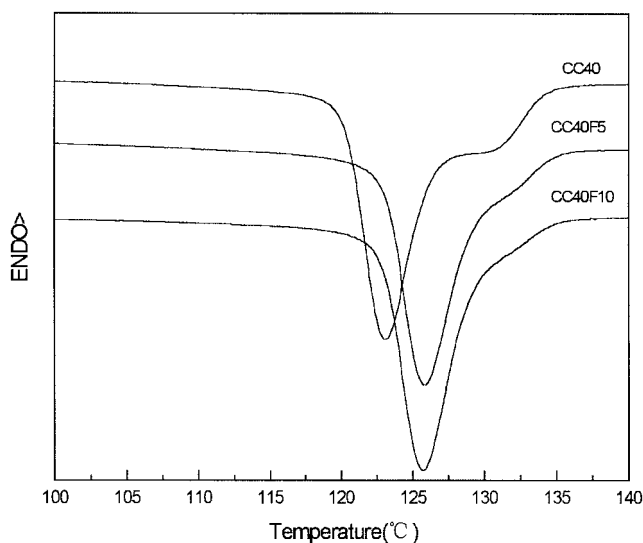


Figure 4 DSC crystallization curves of nano-CaCO₃/PP modified with FPP.

matrix and interface adhesion between nanoparticles and matrix or interface adhesion between particles in the aggregation. Although traditional organic coupling agents improved the dispersion of the filler in the matrix, the improved interface adhesion between the filler and the matrix or between the filler and the filler is limited because the organic chains are short and unreactive. Use of reactive polar monomers, such as acrylic acid, to cover the surface of the filler, and then *in situ* synthesize functionalized macromolecular coupling agent in the preparation process of materials are more effective methods to improve the interface adhesion between filler and matrix.^{1,11,34,45} The macromolecular coupling agent not only can improve the dispersion of the filler in the polymeric matrix, but also strengthen the adhesion between the filler and the polymer matrix. However, there is still no report on nano-CaCO₃/PP composites modified with functionalized macromolecular coupling agents. In our laboratory, the nano-CaCO₃/PP composites modified by AA were prepared by melt mixing in a twin-screw extruder. The nanodispersion of nano-CaCO₃ in PP matrix and improved physical and mechanical properties have been observed.⁴⁶ Physical and mechanical properties of PP composites depend on crystalline morphology of PP, which relates to crystallization be-

havior of PP. Therefore, the effects of additive functionalized PP and *in situ* formed functionalized PP on the crystallization and melting behavior of the nano-CaCO₃/PP composite are investigated in this article.

EXPERIMENTAL

Materials

Pelletized PP (CTS-700) and powdered PP (F-401) were the products of Yinzhu Polypropylene Co. (Guangzhou, China). Nano-calcium carbonate (CaCO₃; particle diameter between 40 and 60 nm; pH 9.6; BET surface area 23.24 m²/g) was obtained from Guangping Chemical Industry Co., China. Chemical-grade acrylic acid (AA), used as the reactive monomer, was purchased from Fushan Chemical Factory, China. Chemical-grade dicumyl peroxide (DCP), used as an initiator for the grafting reaction, was a commercial product of Shanghai Chemical Reagent Factory, China. Premade PP-g-AA (FPP) with grafting yield of 0.56 mol % was synthesized in our laboratory according to the method described in an earlier report.³⁴

Preparation of the PP composite filled with nano-CaCO₃

The composition of nanocomposites is shown in Table I. The AA and DCP were added when nano-CaCO₃ and PP were blended in a GH-10 high-speed mixing machine (Beijing Plastic Machine Factory, China). The mixture was then extruded by a SHJN-20 twin-screw extruder (screw diameter = 25 mm; L/D = 30; Xinli Plastic Machine Factory, Nanjing Aviation University, China) at temperatures of 180–220°C, with the screw speed set at 60 rpm.

DSC analyses

Differential scanning calorimetry (DSC) was performed with a Perkin–Elmer DSC-7 differential scanning calorimeter (Perkin Elmer Cetus Instruments, Norwalk, CT) under a nitrogen atmosphere. The samples were heated from 50 to 220°C at a rate of 100°C/min, held at that temperature for 5 min, then cooled to 50°C at a rate of 10°C/min, and finally heated again to 220°C at the same rate. The crystallization and melting parameters were recorded from the cooling and re-

TABLE IV
DSC Crystallization Results of Nano-CaCO₃/PP Modified with Premade PP-g-AA

Sample	T_c^0 (°C)	T_c^P (°C)	T_c^f (°C)	T_c^n (°C)	ΔH_c (J/g)	ΔT_c^1 (°C)	ΔT_c^2 (°C)	$\Delta T_c^{1/2}$ (°C)
CC40	137.5	123.1	98.2	127.1	111.5	39.3	4.0	4.3
CC40F5	140.4	125.9	100.9	130.0	104.8	39.5	4.2	4.3
CC40F10	139.1	125.7	101.4	129.7	97.0	37.7	4.0	4.0

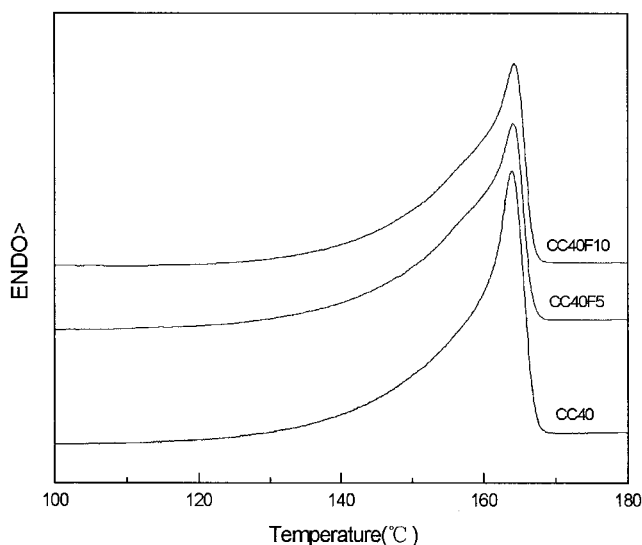


Figure 5 DSC melting curves of nano-CaCO₃/PP modified with FPP.

heating scans. The crystallization and melting parameters were determined according to the method described in Figure 1.

RESULTS AND DISCUSSION

Crystallization and melting behavior of nano-CaCO₃/PP

DSC crystallization curves and data of pure PP and nano-CaCO₃/PP composites are shown in Figure 2 and Table II, respectively. For pure PP, the temperature at which the crystallization curve deviates from the baseline (T_c^0), the peak temperature of crystallization (T_c^P), and the temperature at the onset of crystallization (T_c^{on}) are 128.2, 117.5, and 121.9°C, respectively. When a small amount of nano-CaCO₃ (≤ 5 wt %) is added to PP, the T_c^0 , T_c^P , and T_c^{on} of the nano-CaCO₃/PP (CC2 and CC5) are lower than that of pure PP. When the nano-CaCO₃ is above 10 wt %, the T_c^0 , T_c^P , and T_c^{on} are increased with values much higher than those of pure PP. The increase in the crystallization temperature of PP is more significant with increasing nano-CaCO₃ content. Incorporation of nano-CaCO₃ can cause the width of crystallization peak (ΔT_c^2) in the high temperature region and the half-height width ($\Delta T_c^{1/2}$) of the crystallization peak to

narrow slightly, especially for the system containing 5 wt % nano-CaCO₃. It is suggested that the incorporation of nano-CaCO₃ increases the crystallization rate of PP. The nano-CaCO₃ has only a slight influence on the heat of crystallization of PP (ΔH_c) when the content of nano-CaCO₃ is lower than 10 wt %; on the contrary, the nano-CaCO₃ of 40 wt % increases the ΔH_c .

It is suggested that the high content of nano-CaCO₃ induced a greater heterogeneous nucleation effect and increased the crystallization degree of PP. Moreover, there is a shoulder peak at 129.6°C in the crystallization curve of PP when the content of nano-CaCO₃ is 40 wt %. Evidently, nano-CaCO₃ with high content can greatly change the crystallization behavior of PP. Mitsuishi et al.⁴ also found that there was a shoulder peak or double peak in the DSC curve of CaCO₃/PP composites. They thought that the interaction between polymer and filler changed the crystallization rate of the matrix on the surface of fillers, and accordingly affected the crystallization behavior of PP. After CaCO₃ was treated by alkyl dihydrogen phosphate, the double peak disappeared. They believed that the surface of treated CaCO₃ was covered by treating agents, and therefore decreased the heterogeneous nucleation effect of CaCO₃ on PP. In this study, nano-CaCO₃ was treated by stearic acid. For lower contents of nano-CaCO₃, the effect of nano-CaCO₃ on the melt viscosity of PP is not great, and the friction and shear force during the mixing are too weak to destroy the surfactant covering on the surface of nano-CaCO₃. Because the surface of nano-CaCO₃, which acts as the heterogeneous nucleation agent of PP, is covered by stearic acid, the crystallization temperature of PP is decreased slightly. However, the incorporation of high nano-CaCO₃ contents can increase the melt viscosity of PP, in which the contact probability among nano-CaCO₃ particles and the friction are increased. The stearic acid that coated the surface of CaCO₃ may have been stripped off, and thus the exposed surface of CaCO₃ increases the interfacial interaction between nano-CaCO₃ and PP. Therefore PP has a higher crystallization temperature. Addition of nano-CaCO₃ not only changed the main crystallization peak but also a shoulder peak was observed, attributed to the heterogeneous nucleation.

Figure 3 presents the DSC melting curves of pure PP and nano-CaCO₃ composites and the melting data are

TABLE V
DSC Melting Results of Nano-CaCO₃/PP Modified with Premade FPP

Sample	T_m^0 (°C)	T_m^P (°C)	T_m^f (°C)	T_m^{on} (°C)	ΔH_m (J/g)	ΔT_m (°C)	$\Delta T_m^{1/2}$ (°C)
CC40	113.2	164.0	169.0	158.8	106.8	56.6	6.7
CC40F5	118.0	164.3	169.5	157.4	98.6	51.4	9.1
CC40F10	118.0	164.2	170.0	157.1	93.7	52.0	9.3

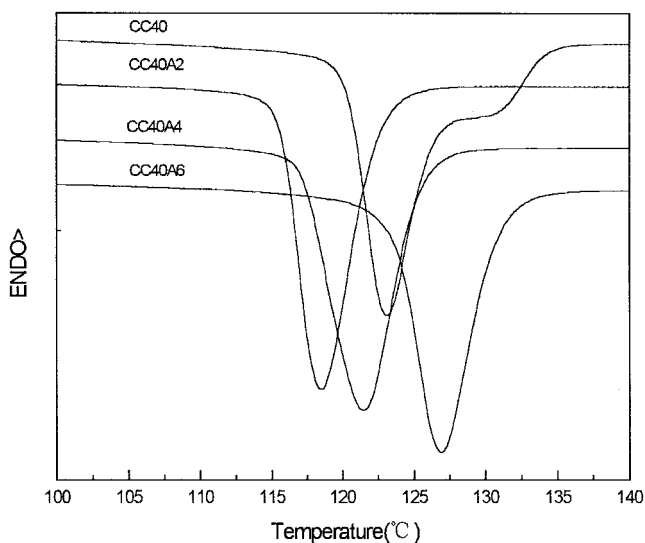


Figure 6 DSC crystallization curves of nano-CaCO₃/PP modified with AA.

shown in Table III. When the content of nano-CaCO₃ is lower (≤ 5 wt %), the melting peak temperature T_m^p , the temperature at the melting completion T_m^f , and the temperature at the melting onset T_m^{on} do not change significantly compared with pure PP. When the content of nano-CaCO₃ is more than 10 wt %, PP filled with nano-CaCO₃ has a high T_m^p , but the T_m^{on} is scarcely changed. The increase of T_m^p is attributed to formation of a more perfect crystal of PP with high lamellar thickness and high melting point attributed to the heterogeneous nucleation of nano-CaCO₃. The incorporation of nano-CaCO₃ causes the half-height width of melting peak ($\Delta T_m^{1/2}$) to become wider, which indicates that the size distribution of crystal grains became narrower. As for CC40 with high crystallization temperature and high nano-CaCO₃ content, the $\Delta T_m^{1/2}$ becomes wider because of the influence of the change of the shape of melting peak. The incorporation of nano-CaCO₃ affects the shape of melting peak of PP. For pure PP, a single melting peak was observed, but the CC2, CC5, and CC10 have a small melting peak at 147.3, 148.2, and 149.7°C, respectively, in the low-temperature region of the main melting peak. As the content of nano-CaCO₃ is increased, the small peak would shift to a higher temperature. For CC10 and CC40 with the higher nano-CaCO₃ content,

this small peak overlaps with the main peak, which makes the $\Delta T_m^{1/2}$ of CC40 much wider. Although Ren³³ found that nano-CaCO₃ could induce PP to form β -crystal and there was a melting peak of β -crystal at about 150°C, it is still expected to further confirm by the experiment reported here whether the small melting peak is related to the formation of β -crystal.

Crystallization and melting behavior of nano-CaCO₃/PP modified with premade PP-g-AA

DSC crystallization curves of nano-CaCO₃/PP composites modified with premade PP-g-AA are shown in Figure 4 and the crystallization data are presented in Table IV. For PP filled with 40 wt % nano-CaCO₃, the T_c^0 , T_c^f , T_c^p , and T_c^{on} are 137.5, 98.2, 123.1, and 127.1°C, respectively. When PP-g-AA of 5 and 10 phf was added, all the above values of the samples were increased but ΔT_c^1 , ΔT_c^2 , and $\Delta T_c^{1/2}$ scarcely changed. Mai et al.³⁴ found that the PP-g-AA can improve the heterogeneous nucleation effect of nano-CaCO₃ and further increase the crystallization temperature. However, ΔH_c decreased with increasing of the PP-g-AA content. The $\Delta T_c^{1/2}$ of the crystallization peak does not obviously change, which indicates that the addition of PP-g-AA has no evident influence on the size distribution of PP crystal grain.

Our studies on Al(OH)₃/PP composites modified with functionalized polypropylene indicated that the PP-g-AA can improve the nucleation of PP and increase the crystallization temperature.³⁵⁻³⁸ In nano-CaCO₃/PP composites modified with PP-g-AA, the promoted heterogeneous nucleation effect of nano-CaCO₃ by PP-g-AA reach a saturation when 5 phf PP-g-AA was added into nano-CaCO₃/PP. When the content of PP-g-AA was increased to 10 phf, the crystallization temperature of PP no longer increases. The incorporation of PP-g-AA can also change the shape of the crystallization peak of PP in the nano-CaCO₃/PP composite. With the increasing of PP-g-AA content, the intensity of the shoulder peak of CC40 at high temperature tends to be weakened. It is suggested that PP-g-AA lies in the interface between nano-CaCO₃ and PP and produces the interaction of the interface between nano-CaCO₃ and PP, thus decreasing the effect of CaCO₃ on the PP crystallization behavior and weakening the intensity of the shoulder peak at high temperature.

TABLE VI
DSC Crystallization Results of Nano-CaCO₃/PP Modified with AA

Sample	T_c^0 (°C)	T_c^p (°C)	T_c^f (°C)	T_c^{on} (°C)	ΔH_c (J/g)	ΔT_c^1 (°C)	ΔT_c^2 (°C)	$\Delta T_c^{1/2}$ (°C)
CC40	137.5	123.1	98.2	127.1	111.5	39.3	4.0	4.3
CC40A2	128.6	118.5	101.6	122.6	96.0	27.0	4.1	4.0
CC40A4	132.0	121.5	100.4	125.5	104.6	31.6	4.0	5.1
CC40A6	137.5	126.9	100.9	130.9	102.4	36.6	4.0	4.3

Figure 5 presents the DSC melting curves of nano-CaCO₃/PP composites modified with premade PP-g-AA and the melting data are shown in Table V. Although the addition of PP-g-AA and the increase in the PP-g-AA content have no significant influence on the T_m^p , T_m^f , and $T_m^{1/2}$, the T_m^{on} and ΔH_m are decreased slightly and the T_m^0 and $\Delta T_m^{1/2}$ are increased with increasing of the PP-g-AA content. It is thought that the addition of PP-g-AA is helpful in causing nano-CaCO₃/PP composites to form crystals with small crystal lamellae and wide crystal size distribution. However, the incorporation of PP-g-AA significantly changes the shape of the melting peak. The intensity of the melting peak in low temperature region is sharply increased.

Crystallization and melting behavior of nano-CaCO₃/PP modified with acrylic acid

DSC crystallization curves of nano-CaCO₃/PP composites modified with acrylic acid (AA) are shown in Figure 6 and crystallization data are presented in Table VI. Addition of 2 phf AA decreased the T_c^0 , T_c^f , and T_c^{on} of PP in nano-CaCO₃/PP composites. However, the T_c^0 , T_c^f , and T_c^{on} gradually increase with increasing AA content. When the AA content is 6 phf, the T_c^0 , T_c^f , and T_c^{on} are higher than those of unmodified nano-CaCO₃/PP composites. For the nano-CaCO₃ used here with particle diameter of 40–60 nm, the specific surface area is about 23.24 m²/g. Assuming that the AA tends to orient normal to the surface of the filler with the carboxylic acid group, then one AA molecule should occupy an area of about 0.2 nm².⁴⁷ The surface area of the nano-CaCO₃ (i.e., 23.24 m²/g) requires 11.62×10^{19} molecules/g or 0.18 mmol/g of AA to form a monolayer coating, which is equivalent to 1.38 phf. Therefore, in other words, the dosage of AA in our work is more than that of the single molecular layer. Tabtiang^{2,11} also found that if the dosage of AA was greater than that of the single molecular layer, the reaction of excessive AA with micro-CaCO₃ produced Ca(AA)₂, which was dissociated in the matrix. In our work, addition of AA with a low content weakened the heterogeneous nucleation effect of nano-CaCO₃ and led to a lower crystallization temperature than that of the unmodified composites because the surface of nano-CaCO₃ is covered with AA. With in-

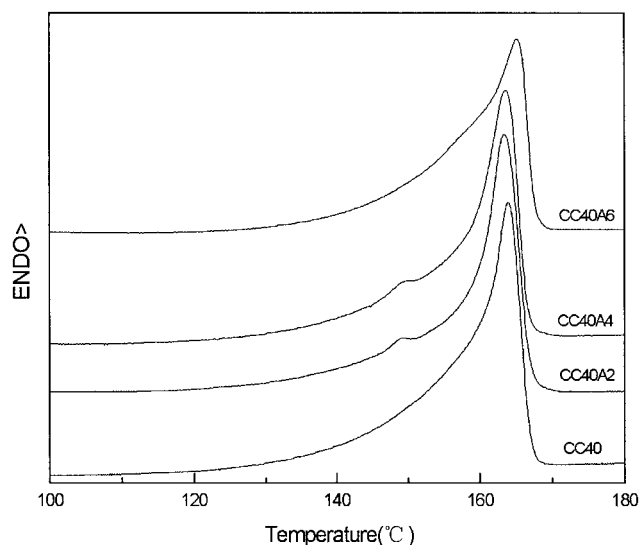


Figure 7 DSC melting curves of nano-CaCO₃/PP modified with AA.

creasing of AA, the excessive AA will react with nano-CaCO₃ to form Ca(AA)₂, which leads to improved heterogeneous nucleation and increased crystallization temperature of PP in nano-CaCO₃/PP composites. Addition of AA decreased the ΔH_c of all samples, although ΔT_c^2 values scarcely changed. The addition of AA also caused the complete disappearance of the shoulder peak in the unmodified sample, the same as with PP-g-AA, which indicates that the heterogeneous nucleation effect of nano-CaCO₃ on the crystallization of PP is weakened because of the surface coverage of nano-CaCO₃ with AA.

Figure 7 presents the DSC melting curves of samples corresponding to Figure 6 and the melting data are shown in Table VII. The addition of AA slightly decreased the T_m^p . However, when AA of 6 phf was added, the T_m^p was higher than that of the sample without AA. It is suggested that the addition of lower content of AA decreases the crystallization temperature of PP in the nano-CaCO₃/PP composites and forms crystals with small lamellar thickness and a lower degree of crystallization perfection. In the nano-CaCO₃/PP composites modified by 6 phf of AA, the lamellar thickness and T_m^p both increased as a result of the higher crystallization temperature. The T_m^0 was

TABLE VII
DSC Melting Results of Nano-CaCO₃/PP Modified with AA

Sample	T_m^0 (°C)	T_m^p (°C)	T_m^f (°C)	T_m^{on} (°C)	ΔH_m (J/g)	ΔT_m (°C)	$\Delta T_m^{1/2}$ (°C)
CC40	113.2	164.0	169.8	158.6	106.8	56.6	6.7
CC40A2	115.9	163.5	171.6	158.5	96.1	55.7	5.3
CC40A4	116.4	163.6	171.2	157.2	101.0	54.8	5.9
CC40A6	121.8	165.3	170.5	157.0	97.3	48.8	9.3

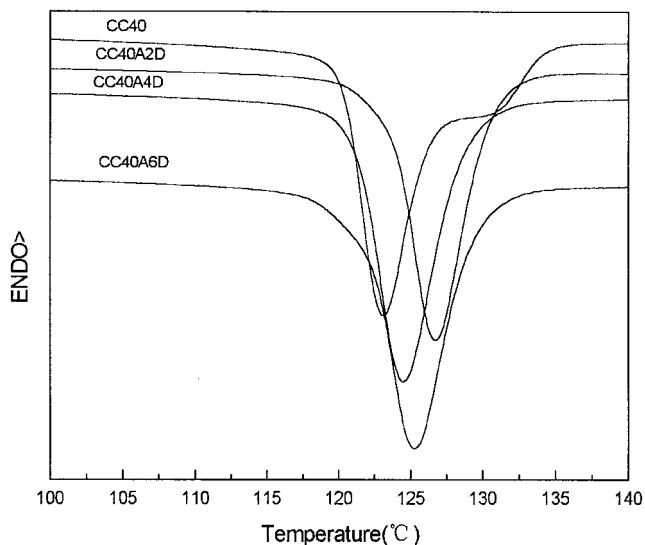


Figure 8 DSC crystallization curves nano-CaCO₃/PP modified with AA in the presence of DCP.

increased with increasing AA content. For the 6 phf of AA, the T_m^0 was 8.6°C higher than that of the sample without AA. The addition of AA also slightly increased T_m^f compared to that of the unmodified sample. However, the incorporation of AA and increasing of the AA content decreased the T_m^{on} because of the change of the peak shape. The effect of AA content on the $\Delta T_m^{1/2}$ was observed. When either 2 and 4 phf AA was added, the $\Delta T_m^{1/2}$ was lower than that of the sample without AA. Addition of 6 phf AA increased the $\Delta T_m^{1/2}$ and the $\Delta T_m^{1/2}$ was 2.6°C higher than that of the sample without AA. The $\Delta T_m^{1/2}$ is related to the change of the peak shape. Compared to the sample without AA, a small peak appeared at temperatures of 148.8 or 149.2°C in the nano-CaCO₃/PP composites modified by 2 and 4 phf AA, respectively. However, the small peak disappeared again and the area of the low-temperature region of the melting peak increased in the nano-CaCO₃/PP composites modified with 6 phf AA. The small melting peak is probably related to the β -crystal of PP, which is expected to be further confirmed by experiments.

Crystallization and melting behavior of nano-CaCO₃/PP modified with AA in the presence of dcp

DSC crystallization curves of nano-CaCO₃/PP composites modified with AA in the presence of DCP are

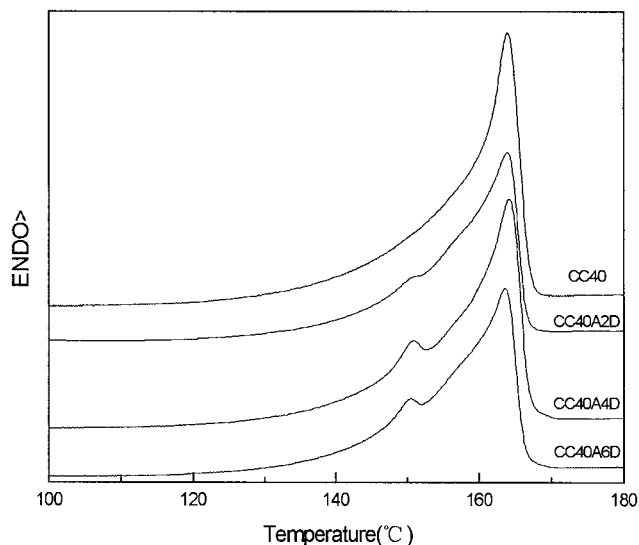


Figure 9 DSC melting curves of nano-CaCO₃/PP modified with AA in the presence of DCP.

shown in Figure 8 and the crystallization data are presented in Table VIII. For the composites containing DCP the objective was to promote coupling through grafting between AA and PP. Compared with Figure 6, the temperature of the crystallization peak of PP in nano-CaCO₃/PP composites modified with AA in the presence of DCP is much higher than that of nano-CaCO₃/PP composites modified only with AA. The T_c^0 , T_c^p , T_c^f , and T_c^{on} of composites modified with 2 phf AA in the presence of DCP are 7.8, 8.2, 5.0, and 3.5°C higher than those of the composites without DCP. As for the composites without DCP, the T_c^0 , T_c^p , and T_c^{on} are increased with increasing AA content. After DCP was added, however, the effect of the AA content on the crystallization temperature decreased. On one hand, the nucleation effect of the formation of *in situ* formed PP-g-AA increases the crystallization rate; on the other hand, the polarity of PP-g-AA hinders the growth of PP crystal. If the effect of CaCO₃ on the PP crystallization is ascertained by increasing the temperature of the crystallization peak, the incorporation of AA with a high content can increase the crystallization peak temperature of PP without DCP; in the presence of DCP, however, only with the content of 2 phf AA can PP obtain a higher crystallization peak temperature. In the meantime, the shape of the crystallization peak also changes and the shoulder peak of

TABLE VIII
DSC Crystallization Results of Nano-CaCO₃/PP Modified with AA in the Presence of DCP

Sample	T_c^0 (°C)	T_c^p (°C)	T_c^f (°C)	T_c^{on} (°C)	ΔH_c (J/g)	ΔT_c^1 (°C)	ΔT_c^2 (°C)	$\Delta T_c^{1/2}$ (°C)
CC40	137.5	123.1	98.2	127.1	111.5	39.3	4.0	4.3
CC40A2D	136.4	126.7	103.2	130.6	100.4	33.2	3.8	3.7
CC40A4D	135.7	124.5	103.2	128.8	111.5	32.5	4.3	4.5
CC40A6D	137.1	125.3	104.1	129.5	99.5	33.0	4.2	4.5

TABLE IX
DSC Melting Results of Nano-CaCO₃/PP Modified with AA in the Presence of DCP

Sample	T_m^0 (°C)	T_m^p (°C)	T_m^f (°C)	T_m^{on} (°C)	ΔH_m (J/g)	ΔT_m (°C)	$\Delta T_m^{1/2}$ (°C)
CC40	113.2	164.0	169.8	158.6	106.8	56.6	6.7
CC40A2D	111.8	164.0	169.3	154.3	93.8	57.5	9.1
CC40A4D	120.7	164.2	171.6	157.3	108.9	50.9	8.0
CC40A6D	120.7	163.7	170.5	155.1	93.8	49.8	9.3

CC40 disappears. In the presence of DCP, the effect modified with AA is similar to that modified with PP-g-AA. The formation of *in situ* formed PP-g-AA lies in the interface between nano-CaCO₃ and PP, which affects the crystallization behavior of nano-CaCO₃-filled PP.

Figure 9 presents the DSC melting curves of samples corresponding to Figure 8 and the melting data are shown in Table IX. In the presence of DCP, the T_m^p , T_m^f , T_m^{on} , and ΔH_m scarcely change but $\Delta T_m^{1/2}$ is widened. The formation of *in situ* formed PP-g-AA in the presence of DCP promotes the nucleation and accelerates the crystallization of PP, although the polarity interaction of PP-g-AA hinders the growth of PP crystal and widens the size distribution of crystal lamellae. From Figure 8, a small peak at about 150°C, which is not affected by the content of AA, may be observed that may be related to the β -crystal of PP. For the same content of AA, the intensity of the small melting peak of PP increases in the composites modified with AA in the presence of DCP. It is suggested that the scission of PP chains in the presence of DCP decreases the molecular weight and increases the ability to produce β -crystal.

CONCLUSIONS

A low content of nano-CaCO₃ did not exert a nucleation effect on PP to increase the crystallization temperature of PP because of the coating of stearic acid. With a high content of nano-CaCO₃, however, the coating of stearic acid was stripped off during the preparation of nano-CaCO₃/PP composites in the extruder; the exposed surface of nano-CaCO₃ exerted a heterogeneous nucleation effect on PP, leading to an increase of crystallization temperature. With the increased content of AA, the crystallization temperature of nano-CaCO₃/PP composites modified by acrylic acid (AA) was increased because of the formation of Ca(AA)₂. In the presence of DCP, the nano-CaCO₃/PP modified by AA also had a higher crystallization temperature because of the formation of PP-g-AA. According to the change of crystallization and melting behavior, we deduced that the modification of AA with and without DCP mainly existed on the interface and led to the change of interface interaction between

nano-CaCO₃ and PP, consequently influencing the other important properties, thus providing a compelling basis for further investigation.

References

- Kowalewski, T.; Galeski, A. *J Appl Polym Sci* 1986, 32, 2919.
- Tabtiang, A.; Venables, R. *Plast Rubber Compos Process Appl* 1999, 28, 11.
- Yang, J.; Liu, W.; Chen, G.; Liu, J. *Acta Polym Sinica* 2001, 3, 383 (in Chinese).
- Mitsuiishi, K.; Ueno, S.; Kodama, S.; Kawasaki, H. *J Appl Polym Sci* 1991, 43, 2043.
- Khare, A.; Mitra, A.; Radhakrishnan, S. *J Mater Sci* 1996, 31, 5691.
- Tjong, S. C.; Xu, S. A. *Polym Int* 1997, 44, 95.
- Albano, C.; Gonzalez, J.; Ichazo, M.; Rosales, C.; Navarro, C. U.; Parra, C. *Comp Struct* 2000, 48, 49.
- Ren, Z.; Shanks, R. A.; Rook, T. J. *J Appl Polym Sci* 2001, 79, 1942.
- Akovi, G.; Akmant, M. A. *Polym Int* 1997, 42, 195.
- Rahma, F.; Fellahi, S. *Polym Compos* 2000, 21, 175.
- Tabtiang, A.; Venables, R. *Eur Polym Mater* 2000, 36, 137.
- LeBaron, P. C.; Wang, Z.; Pinnavaia, T. J. *Appl Clay Sci* 1999, 15, 11.
- Michael, A.; Philippe, D. *Mater Sci Eng* 2000, 28, 1.
- Kathleen, A. C. *Appl Clay Sci* 2000, 17, 1.
- Gilman, J. W.; Jackson, C. L.; Morgan, A. B.; Harris, R.; Manias, E.; Giannelis, E. P.; Wuthenow, M.; Hilton, D.; Phillips, S. H. *Chem Mater* 2000, 12, 1866.
- Zanetti, M.; Lomakin, S.; Camino, G. *Macromol Mater Eng* 2000, 12, 1866.
- Burnside, S. D.; Giannelis, E. P. *J Polym Sci Part B: Polym Phys* 2000, 38, 1595.
- Gardolinski, J. E.; Carrera, L. C. M.; Cantao, M. P.; Wypych, F. *J Mater Sci* 2000, 35, 3113.
- Porter, D.; Metcalfe, E.; Thomas, M. J. K. *Fire Mater* 2000, 24, 45.
- Gangopadhyay, De, A. R. *Chem Mater* 2000, 12, 608.
- Garcks, J. M.; Moll, D. J.; Bicerano, J.; Fibiger, R.; McLead, D. G. *Adv Mater* 2000, 12, 1835.
- Sun, T.; Garces, J. M. *Adv Mater* 2002, 14, 128.
- Zhu, J.; Start, P.; Mauritz, K. A.; Wilkie, C. A. *J Polym Sci Part A: Polym Chem* 2002, 40, 1498.
- Jyh, M. H.; Jiang, G. J.; Zong, M. G.; Xie, W.; Wei, P. P. *J Appl Polym Sci* 2002, 83, 1702.
- Masenelli-Varlot, K.; Reynaud, E.; Vigier, G.; Varlet, J. *J Polym Sci Part B: Polym Phys* 2002, 40, 272.
- Liu, X.; Wu, Q. *Eur Polym Mater* 2002, 38, 1383.
- Xu, W.; Ge, M.; He, P. *J Polym Sci Part B: Polym Phys* 2002, 40, 408.
- Ma, J.; Qi, Z.; Li, G.; Hu, Y. *Acta Polym Sinica* 2001, 5, 589 (in Chinese).
- Ma, J.; Zhang, S.; Qi, Z.; Li, G.; Hu, Y. *J Appl Polym Sci* 2002, 83, 1978.
- Wu, W.; Xu, Z. *Acta Polym Sinica* 2000, 1, 100 (in Chinese).

31. Saujanya, C.; Radhakrishnan, S. *Polymer* 2001, 42, 6723.
32. Wang, X.; Huang, R. *China Plast* 1999, 13, 22 (in Chinese).
33. Ren, X.; Bai, L.; Wang, G. *China Plast* 2000, 14, 22 (in Chinese).
34. Mai, K.; Li, Z.; Zeng, H. *J Appl Polym Sci* 2001, 80, 2609.
35. Mai, K.; Li, Z.; Qiu, Y.; Zeng, H. *J Appl Polym Sci* 2001, 80, 2617.
36. Mai, K.; Li, Z.; Qiu, Y.; Zeng, H. *J Appl Polym Sci* 2001, 81, 2679.
37. Mai, K.; Li, Z.; Qiu, Y.; Zeng, H. *J Appl Polym Sci* 2002, 83, 2850.
38. Mai, K.; Li, Z.; Zeng, H. *J Appl Polym Sci* 2002, 84, 110.
39. Chiang, W.; Hu, C. *J Polym Res* 2000, 7, 5.
40. Qiu, W.; Mai, K.; Zeng, H. *J Appl Polym Sci* 2000, 77, 2974.
41. Bogoeva-Gaceva, G.; Janevski, A.; Maeder, E. *J Adhes Sci Technol* 2000, 14, 363.
43. Jarvela, P.; Stenlund, B.; Wilen, C. E.; Nicolas, R.; Etelaaho, P. *J Appl Polym Sci* 2002, 84, 1203.
44. Bikiaris, D.; Matzinos, P.; Larena, A.; Flaris, V.; Panayiotou, C. *J Appl Polym Sci* 2001, 81, 701.
45. Ma, Z.; Zhao, M.; Hu, H.; Ding, H.; Zhang, J. *J Appl Polym Sci* 2002, 83, 3128.
46. Lin, Z.; Chen, X.; Huang, Z.; Mai, K. *J Appl Polym Sci*, to appear.
47. Favis, B. D.; Blanchard, L. P.; Leonard, J.; Prud'homme, R. E. *J Appl Polym Sci* 1983, 28, 1235.